Bulletin of the Earthquake
Research Institute
Vol. 49 (1971), pp. 33-62

4. Crustal Structure from Travel Times of Reflected and Refracted Seismic Waves recorded at Wakayama Micro-earthquake Observatory and its Substations.

By Megumi Mizoue,
Earthquake Research Institute.

(Read in March 24, 1970 and June 23, 1970.—Received November 30, 1970.)

Abstract

Travel time analysis is made for deep crustal reflections in the Kii Peninsula on the basis of the observational data detected at Wakayama Micro-earthquake Observatory, E.R.I. (Earthquake Research Institute). Time distance data of direct and refracted waves are correlated with the data of reflections to evaluate seismic wave velocities in the earth's crust.

An interpretation of the time distance data is represented for the reflections from the Conrad and the Mohorovičić discontinuities. The depth of the Conrad discontinuity can be measured as 20-24 km in the western part of the Kii Peninsula with a possible inclination dipping to the west. The depth of the Mohorovičić discontinuity can be estimated as about 30 km in the inland area of the Kii Peninsula. Seismic wave velocities in the upper and the lower crustal layers are estimated as 5.80 km/sec and 6.80 km/sec for the *P*-waves and 3.46 km/sec and 4.05 km/sec for the *S*-waves respectively. The velocities of the *Pg* and *Pn* waves are determined as 5.8 km/sec and 7.9 km/sec respectively from the network observations at the observatory.

Introduction

The observation network of Wakayama Micro-earthquake Observatory of E.R.I., the University of Tokyo, which covers the whole area of the Kii Peninsula, Central Japan, consists of 11 stations with high magnification short period seismographs. Station locations are given in a map (Fig. 1) and are listed in Table 1 together with the elevations. Fig. 2 shows the overall frequency characteristics of the seismographs at the stations. Magnifications and sensitivities of the seismographs are listed in Table 2.

Detailed investigations of seismicity in the Kii Peninsula were made by S. Miyamura[1)-4)], and K. Tsumura[5),6)] with special reference

1) S. Miyamura, "Local earthquakes in Kii Peninsula, Central Japan. Part 1. Reconnaissance observation of minor shocks at Gobo, Wakayama Prefecture," *Bull. Earthq. Res. Inst.*, **37** (1959), 347-358.

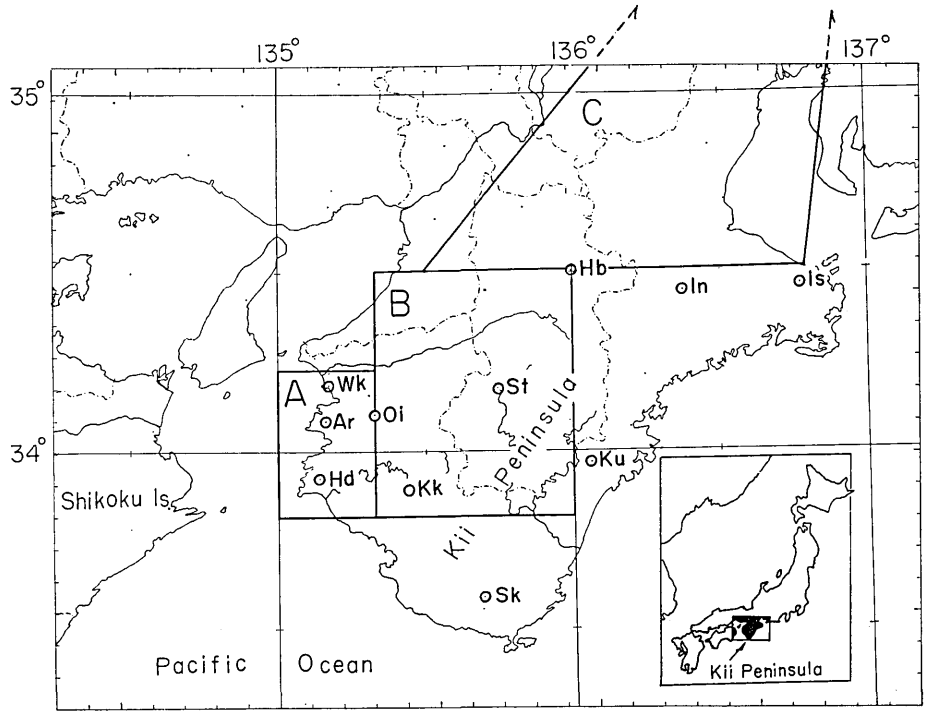

Fig. 1. Locations of stations and zones.

to the local earthquake activities in the neighbourhood of Wakayama city. Results of the routine observations were summarized in the Seismological Bulletins of the observatory for 1965[7)–9)]. Preliminary

2) S. MIYAMURA, "Local earthquakes in Kii Peninsula, Central Japan. Part 2. A brief review of seismicity in Wakayama Prefecture based on intensity investigations," *Bull. Earthq. Res. Inst.*, **37** (1959), 593-608.

3) S. MIYAMURA, "Local earthquakes in Kii Peninsula, Central Japan. Part 3. Temporary seismological network in the neighbourhood of Wakayama," *Bull. Earthq. Res. Inst.*, **37** (1959), 609-635.

4) S. MIYAMURA, "Local earthquakes in Kii Peninsula, Central Japan. Part 4. Location of earthquakes by temporary network of stations near Wakayama," *Bull. Earthq. Res. Inst.*, **37** (1960), 71-112.

5) K. TSUMURA, "Development of aftershock area of small earthquakes estimated from difference of P arrival times." *Read at the meeting of Seism. Soc. Japan, Nov.* 14, 1968.

6) K. TSUMURA, "Detection of anomalous seismic activity from frequency of earthquakes within narrow $S-P$ time range," *Read at the meeting of Seism. Soc. Japan, Nov.* 1969.

7) Wakayama Micro-earthquake Observatory, Earthq. Res. Inst., *Seismological Bulletin of Wakayama Micro-earthquake Observatory and its Substations*, January-June, 1965.

8) Wakayama Micro-earthquake Observatory, Earthq. Res. Inst., *Seismological Bulletin of Wakayama Micro-earthquake Observatory and its Substations*, July-September, 1965.

9) Wakayama Micro-earthquake Observatory, Earthq. Res. Inst., *Seismological Bulletin of Wakayama Micro-earthquake Observatory and its Substations*, October-December, 1965.

Table 1. List of stations of Wakayama Micro-earthquake Observartory (The coordinates of X and Y are measured in km as positive to the east and to the north from the origin of 135°E and 34°N.)

Station	Abbr.	Longitude	Latitude	Elevation	X	Y
Wakaura	Wk	135.1730	34.1879	11 m	15.94	20.85
Oishiyama	Oi	135.3273	34.1053	678	30.20	11.73
Arida	Ar	135.1617	34.0859	41	14.93	9.54
Kainokawa	Kk	135.4418	33.8987	256	40.87	−11.14
Shichikawa	Sk	135.6908	33.5877	155	64.12	−45.52
Sarutani	St	135.7460	34.1762	470	68.77	19.79
Haibara	Hb	135.9933	34.5028	390	91.21	56.21
Iinan	In	136.3748	34.4463	155	126.32	50.35
Ise	Is	136.7740	34.4585	440	162.97	52.28
Kumano	Ku	136.0582	33.9677	300	97.79	− 3.08
Hidaka	Hd	135.1390	33.9259	30	12.85	− 8.21

Table 2. Magnifications ($\times 10^3$ at 1Hz) and sensitivities (cm kine at 10 Hz) at the stations of Wakayama Micro-earthquake Observatory

Station	Comp.	Mag.	Sens.	Station	Comp.	Mag.	Sens.
Wk	Z	5.8	630	Sk	Z	9.7	1400
	N	3.7	440	St	Z	16	2600
	E	3.7	440	Hb	Z	16	2600
Oi	Z	16	2100	In	Z	10	1700
	N	5.0	800	Is	Z	19	3000
Ar	Z	14	2000	Ku	Z	15	2400
Kk	Z	17	2300	Hd	Z	6.5	1000

results of the determinations of epicenters and magnitude values for the events detected by the network observations are available in a form of computer outputs for the period 1966–1969.

Three components observation at Wk (Wakaura) station registers about 700 or more events per month including microearthquakes at very close distance (S minus P interval$\leq$2.5 sec). It is a remarkable fact that the events with concentrated epicenters in the neighbourhood of Wakayama city have their focal depths mostly restricted to 5–7 km. It is a rare case for their focal depths to exceed 9 km. A sharp later arrival, which follows the direct S-waves by about 5–11 seconds, is recorded at Wk and Oi (Oishiyama) stations for the nearby earthquakes (S minus P interval $\leq$4.0 sec). The later arrival can be identified as the reflections from the Conrad discontinuity at depth of 20–24 km.

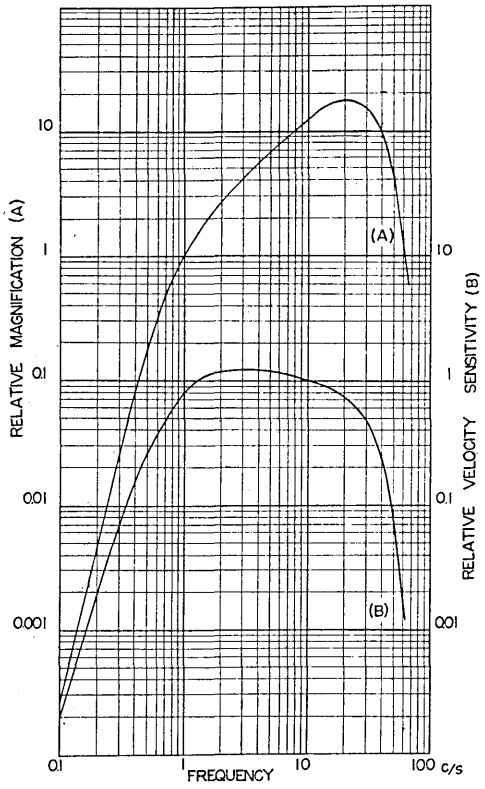

Fig. 2. Overall frequency characteristics of seismographs.

Crustal reflections at very small distance were reported by A. Kamitsuki[10] and A. R. Sanford and L. T. Long[11]. Kamitsuki discussed and reported seismograms of four shocks that have identifiable S phase 'Moho' reflections at epicentral distance ranging 4.0 -11.5 km. Sanford, et al. found late phases which can be identifiable as the SxP and SxS reflections from a crustal discontinuity at a depth of 18 km and at epicentral distance ranging from 4 to 8 km for the microearthquakes which originated close to Socorro, New Mexico. As pointed out by Sanford, et al., it will be notable that observations of crustal reflections at very small distance are apparently quite rare.

In this paper, time distance data were analyzed in special concern to the crustal P and S reflections from the Conrad and the Mohorovičić discontinuity. Some of the seismograms with prominent reflected phases are reproduced from the herical drum records with a paper speed of 4 mm/sec. Error of time readings of initial onset is within the limit of 0.05 sec. Earthquakes used are located assuming a uniform distribution of velocity beneath all stations at which the initial onset is expected to be the direct P phase. The origin time of each event is calculated from the relation between the P and the S minus P interval through the least square procedure. Hypocentral coordinates are determined using the initial P time at four stations which consist of a closely spaced network. The epicentral coordinates thus obtained are within a limit of error of 1.5 km as deduced from the reading error of time of the initial onset.

10) A. KAMITSUKI, "On seismic waves reflected at the Mohorovičić discontinuity (1)," *Mem. Coll. Sci., Univ. Kyoto, Ser. A.*, **28** (1965), 143-159.

11) A. R. SANFORD and L. T. LONG, "Micro-earthquake crustal reflections, Socorro, New Mexico," *Bull. Seism. Soc. Amer.*, **55** (1965), 579-586.

Reflections from the Conrad Discontinuity

Time distance relations of the reflections from the Conrad discontinuity are investigated on the basis of the observational data obtained at the stations of Wakayama Micro-earthquake Observatory. The P and S reflections, denoted as PxP and SxS, are detected at the subcritical and critical distance ranges. Travel time curves of the PxP and SxS phase are interpreted in terms of the depth of the Conrad discontinuity and the averaged velocities of the P and S waves in the upper crustal layer from the earth's surface to the depth of the Conrad discontinuity. The critical distance Δ_1, at which an increase in amplitudes of the reflections may be expected, is estimated from both travel time and amplitude information.

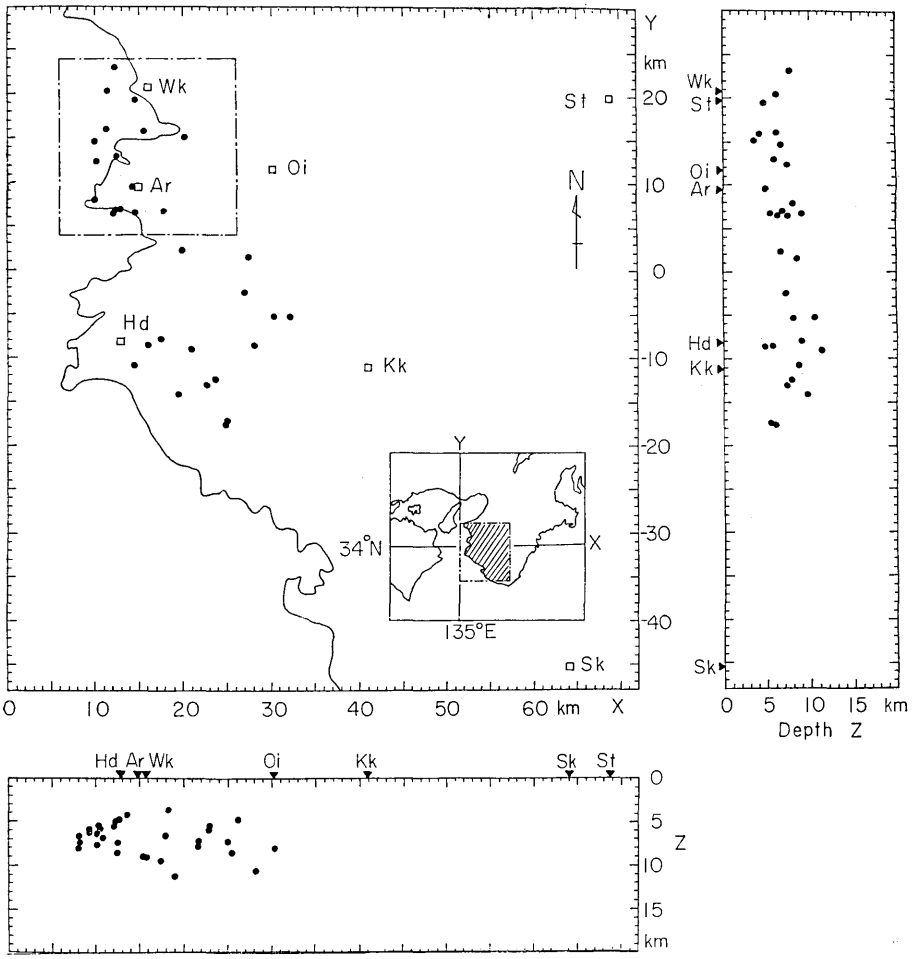

Fig. 3. Hypocentral distributions of earthquakes in Table 3.

Table 3. List of earthquakes used for the travel time analysis of $S-P$ times. (Epicentral coordinates of X and Y are measured origin of 135°E and 34°N. Focal depth measured in km is

No.	Date	Origin Time			Hypocentral Coordinates (km)		
		h	m	s	X	Y	Z
1	May 18, 1969	10	14	40.97	14.58	19.40	4.69
2	June 06, 1969	13	01	19.23	15.55	15.77	4.17
3	Aug. 29, 1969	18	31	58.08	20.23	15.16	3.60
4	Jan. 11, 1968	20	22	32.82	11.29	20.38	6.19
5	Feb. 02, 1969	01	16	49.15	11.25	16.02	6.08
6	Aug. 07, 1969	21	25	39.33	12.54	12.89	5.78
7	Sep. 28, 1969	20	08	30.90	10.20	12.29	7.35
8	Jan. 17. 1967	07	20	17.71	9.97	14.55	6.66
9	Apr. 29, 1967	06	46	08.14	14.28	9.48	4.87
10	Apr. 21, 1969	22	53	16.10	12.93	6.84	6.77
11	Jan. 29, 1969	16	52	39.66	12.27	6.61	5.37
12	Dec. 29, 1967	22	00	10.05	10.03	7.76	8.04
13	Apr. 18, 1969	07	23	29.26	12.18	6.39	6.29
14	May 26, 1969	23	15	12.23	30.32	− 5.28	10.47
15	May 31, 1969	14	35	11.09	12.20	22.97	7.71
16	Feb. 05, 1969	11	46	01.75	17.55	− 8.04	8.96
17	Feb. 19, 1969	17	57	10.98	14.52	−10.88	8.58
18	May 20, 1969	12	05	24.30	19.46	−14.23	9.46
19	Feb. 19, 1969	10	04	21.79	24.88	−17.68	5.87
20	Mar. 22, 1969	00	50	50.38	25.02	−17.52	5.39
21	Apr. 12, 1969	22	26	58.29	32.31	− 5.37	8.05
22	Apr. 26, 1969	17	58	22.59	27.45	1.44	8.05
23	Feb. 10, 1969	07	02	12.09	26.97	− 2.24	7.17
24	Jan. 14, 1969	19	17	05.28	28.14	− 8.63	4.72
25	June 09, 1965	10	16	11.43	19.97	2.21	6.61
26	May 01, 1969	00	59	32.02	23.72	−12.47	7.75
27	Apr. 13, 1965	13	32	19.79	17.78	6.70	8.96
28	Jan. 19, 1969	01	48	47.49	20.96	− 9.12	11.15
29	Jan. 25, 1968	21	36	52.58	22.74	−13.16	7.20
30	Dec. 23, 1965	23	29	00.27	16.07	− 8.63	5.47
31	Mar. 12, 1968	16	34	38.45	14.47	6.37	7.37
10	Apr. 21, 1969	22	53	16.10	12.93	6.84	6.77
9	Apr. 29, 1967	06	46	08.14	14.28	9.48	4.87
11	Jan. 29, 1969	16	52	39.66	12.27	6.61	5.37
13	Apr. 18, 1969	07	23	29.26	12.18	6.39	6.29

The list of 31 earthquakes used for the travel time analysis is arranged in order of the S minus P interval which is used as a measure of epicentral distance as listed in Table 3. Epicentral distributions and

the Conrad reflections of PxP and SxS as arranged in order of in km as positive to the east and to the north respectively from the denoted as Z.)

Mag.	Station	$S-P$ in sec	Travel Time in sec			
			$P-O$	$S-O$	$PxP-O$	$SxS-O$
3.4	Wk	0.60	0.97	1.57		11.47
3.0	Wk	0.83	1.20	2.03		12.60
3.2	Wk	0.95	1.47	2.42		11.69
3.2	Wk	0.99	1.42	2.41		11.82
3.1	Wk	1.20	1.69	2.89		12.09
2.8	Wk	1.32	1.79	3.11		11.79
3.1	Wk	1.32	2.24	3.56		12.11
3.0	Wk	1.38	2.10	3.48		12.60
3.1	Wk	1.55	2.49	4.04		12.99
3.3	Wk	1.91	2.96	4.87		13.01
3.5	Wk	1.92	2.89	4.81		13.59
3.1	Wk	2.03	3.11	5.04		13.13
3.4	Wk	2.13	3.20	5.33		13.70
2.1	Oi	2.36	3.60	5.96		12.35
1.9	Oi	2.75	4.35	7.10		12.35
2.1	Oi	3.10	4.75	7.85		13.55
2.6	Oi	3.40	5.24	8.64		14.24
1.9	Oi	3.47	5.38	8.85		13.78
2.0	Oi	3.75	5.31	9.06		14.41
3.9	Wk	4.50	6.84	11.34	9.24	15.24
2.5	St	5.06	7.64	12.70	9.24	15.64
2.7	St	5.20	7.69	12.89	9.43	15.94
2.2	St	5.44	8.17	13.61	9.92	16.77
1.9	St	5.69	8.29	13.98	9.84	16.74
2.3	St	6.00	8.83	14.83	10.38	17.46
2.0	St	6.35	9.43	15.78	10.53	17.68
2.5	St	6.45	9.57	16.02	10.87	18.46
2.0	St	6.60	9.81	16.41	11.01	18.21
2.0	St	6.62	9.82	16.44	10.86	18.43
1.7	St	6.80	9.92	16.72	11.12	18.91
2.6	St	7.00	10.19	17.19	11.94	20.04
3.3	St	7.12	10.24	17.36	12.23	20.49
3.1	St	7.25	9.85	17.10	12.19	20.25
3.5	St	7.39	10.24	17.63	12.22	20.64
3.4	St	7.50	10.55	18.05	12.55	21.15

focal depths of these earthquakes are plotted in Fig. 3. Prominent reflections are detected at the next three stations of Wk, Oi and St (Sarutani). The S minus P interval of the earthquakes used is in the

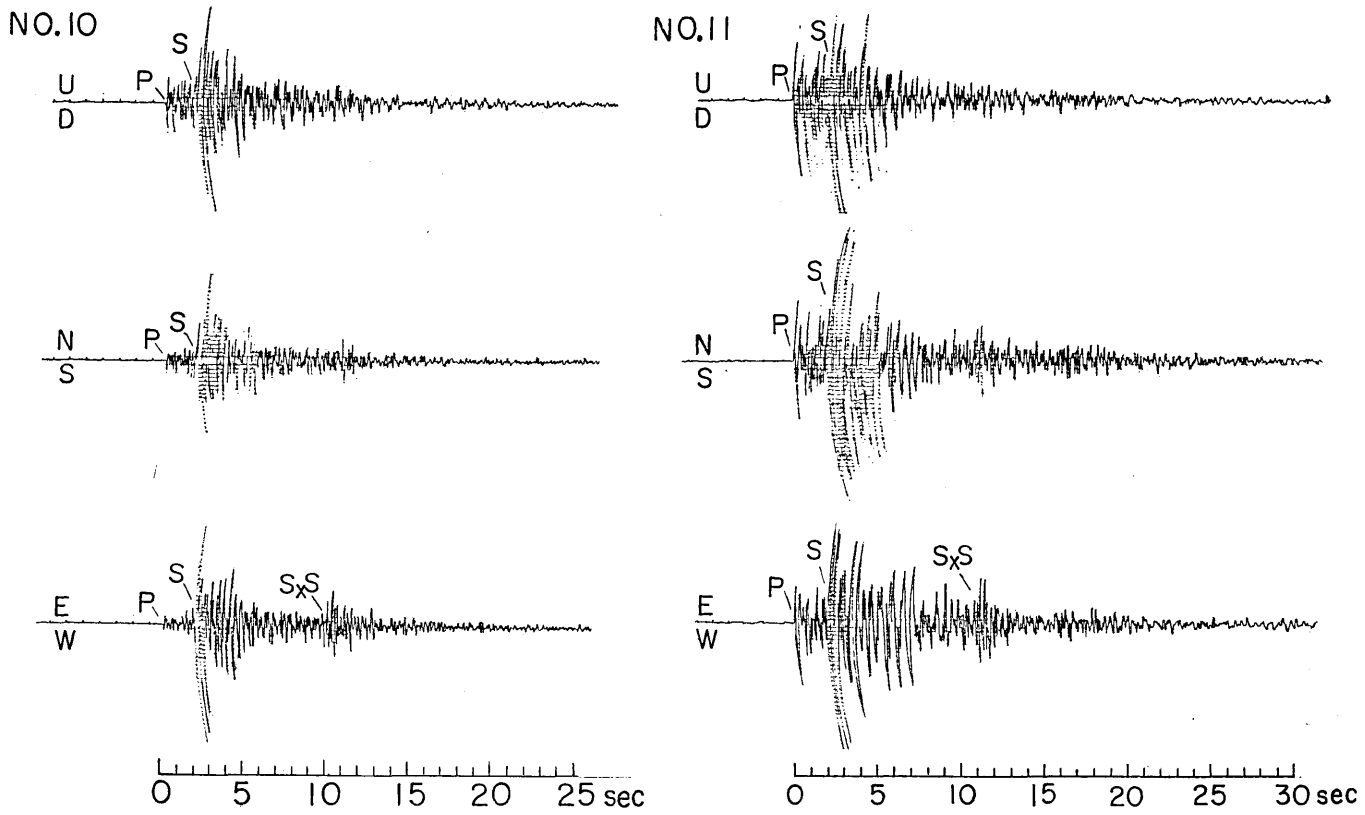

Fig. 4. Three components seismograms at Wakaura station reproduced from the herical drum records with paper speed of 4 mm/sec. The *S* reflections from the Conrad discontinuity are denoted as *SxS*. Numbers for the reproduced seismograms correspond to those in Table 3.

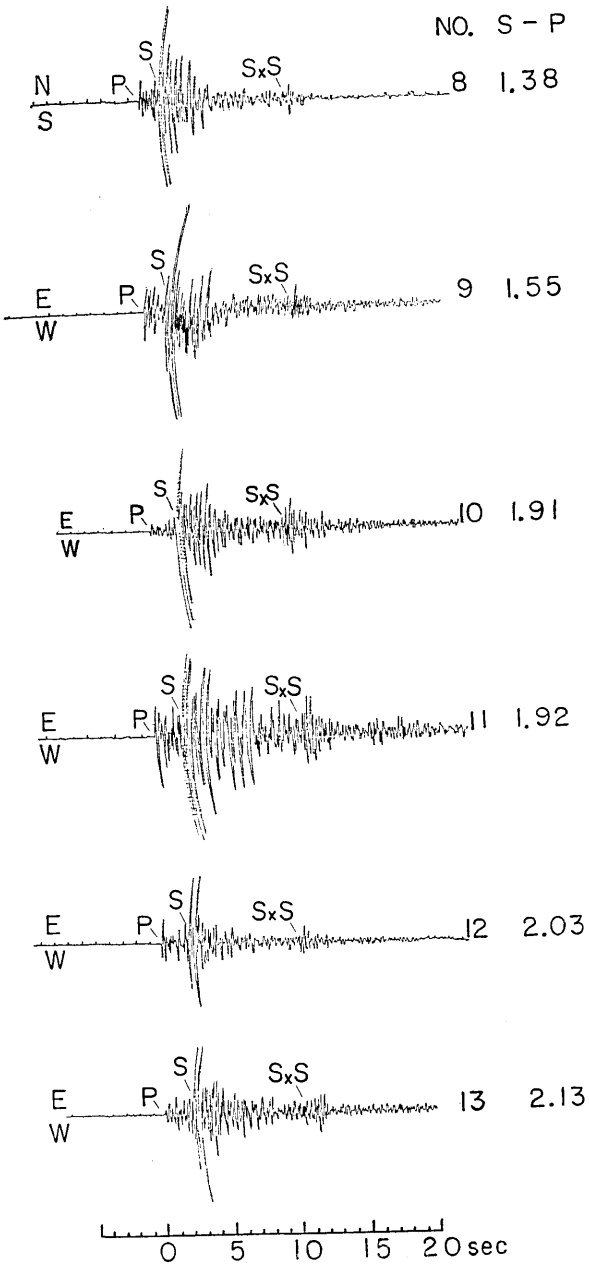

Fig. 5. Horizontal component seismograms at Wakaura station produced from the herical drum records with paper speed of 4 mm/sec. The *S* reflections from the Conrad discountinuity are denoted as *SxS*. Numbers for the reproduced seismograms correspond to those in Table 3.

range of 0.6–7.5 seconds. The focal depth of these earthquakes is in the range of 4–12 km.

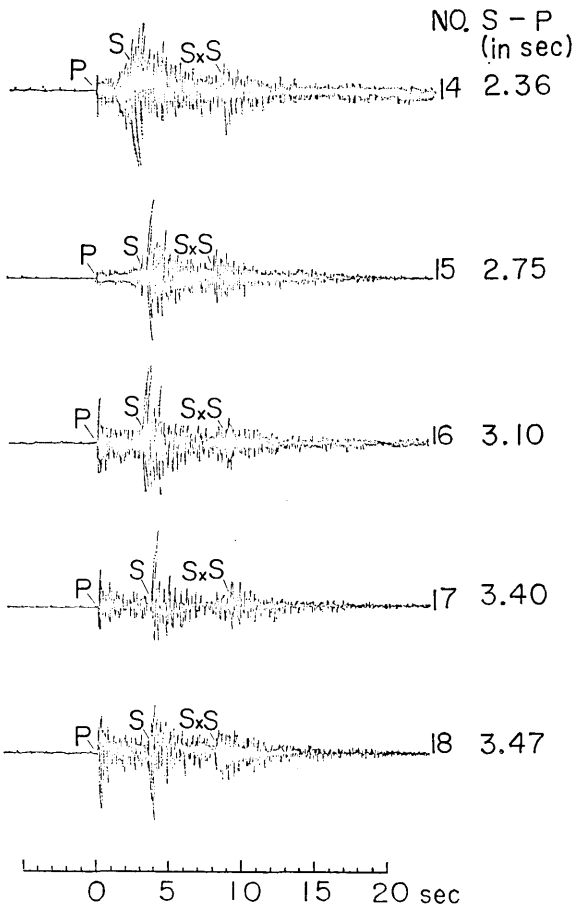

Fig. 6. Horizontal (NS) component seismograms at Oishiyama station reproduced from the herical drum records with paper speed of 4 mm/sec. The *S* reflections from the Conrad discontinuity are denoted as *SxS*. Numbers for the reproduced seismograms correspond to these in Table 3.

In addition to the direct *P* and *S* phases, the nearby earthquakes (*S* minus *P* interval$\leq$4.0 sec) recorded at Wk and Oi stations have a sharp arrival which follows the direct *S* by about 5–11 seconds. Seismograms are reproduced in Figs. 4, 5 and 6 from the original herical drum records at Wk and Oi stations. It is notable that, as shown in Fig. 4, the later phase can be found prominently on the horizontal component seismograms rather than on the vertical ones. The fact suggests that the later arrival can be interpreted as the deep crustal reflections of the *S* waves. Although the direct *S* amplitudes are saturated in most cases for the nearby earthquakes with the later phase with amplitudes large enough to detect, the amplitudes of the later phase can be estimated to be less than 0.13 and 0.25 of the direct *S*

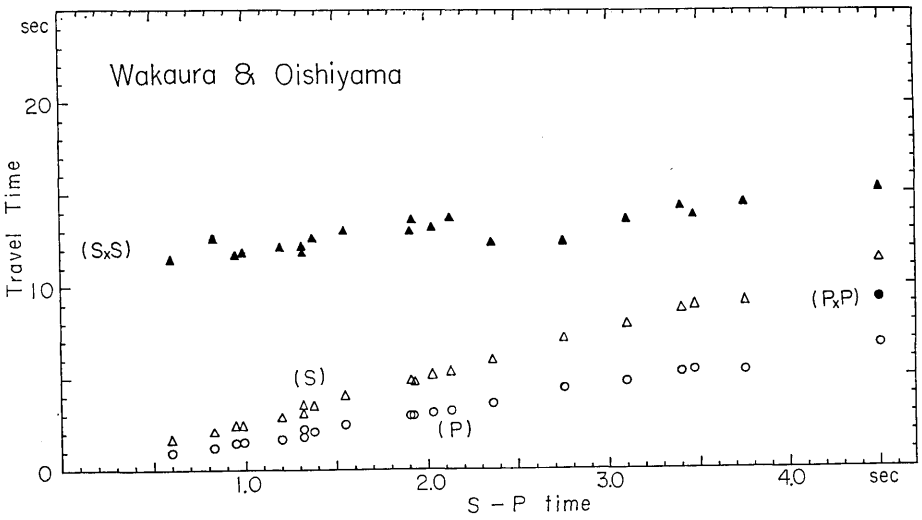

Fig. 7. Observed travel times of *P*, *S*, *PxP* and *SxS* versus *S*−*P* time relations at Wakaura and Oishiyama stations.

amplitude at Wk and Oi stations respectively. Seismograms with the later arrival recorded at Wk and Oi stations are reproduced and arranged in order of the *S* minus *P* interval as shown in Figs. 5 and 6. The travel times versus *S* minus *P* interval relations are given in Fig. 7 for the direct *P*, *S* and the later phase in the close distance range of the *S* minus *P* interval of 0.6–4.0 seconds. From the travel time and distance relations, the later arrival can be identified as the subcritical *S* reflections denoted as *SxS* from the Conrad discontinuity at a depth of 24 km. Detailed interpretation of the travel time curves will be made in the following parts of this section.

In regard to the time distance relations of the reflections from the Conrad discontinuity for the larger distance range of the *S* minus *P* interval of 4.5–7.5 seconds, it should be noted that the earthquakes recorded at Wk and St stations have two sharp arrivals, in addition to the direct *P* and *S* phases, identified as the reflections of the *PxP*, which follow the direct *P* by about 1.0–2.4 seconds, and *SxS*, which follow the direct *S* by about 1.9–3.9 seconds, in the close distance range of the *S* minus *P* interval of less than 4.0 seconds. Seismograms are reproduced in Fig. 8 from the original herical drum records of the vertical component seismograph at St station. The amplitudes of the reflections average 0.6 and 1.5 of those of the direct waves for both the *P* and *S* waves as measured on the vertical component seismograms at St station. In the range of 4.5–7.5 seconds of the *S* minus *P* interval, the amplitude ratio of the reflections to the direct waves is more than 5 times that in the range of the *S* minus *P* interval less than 4.0

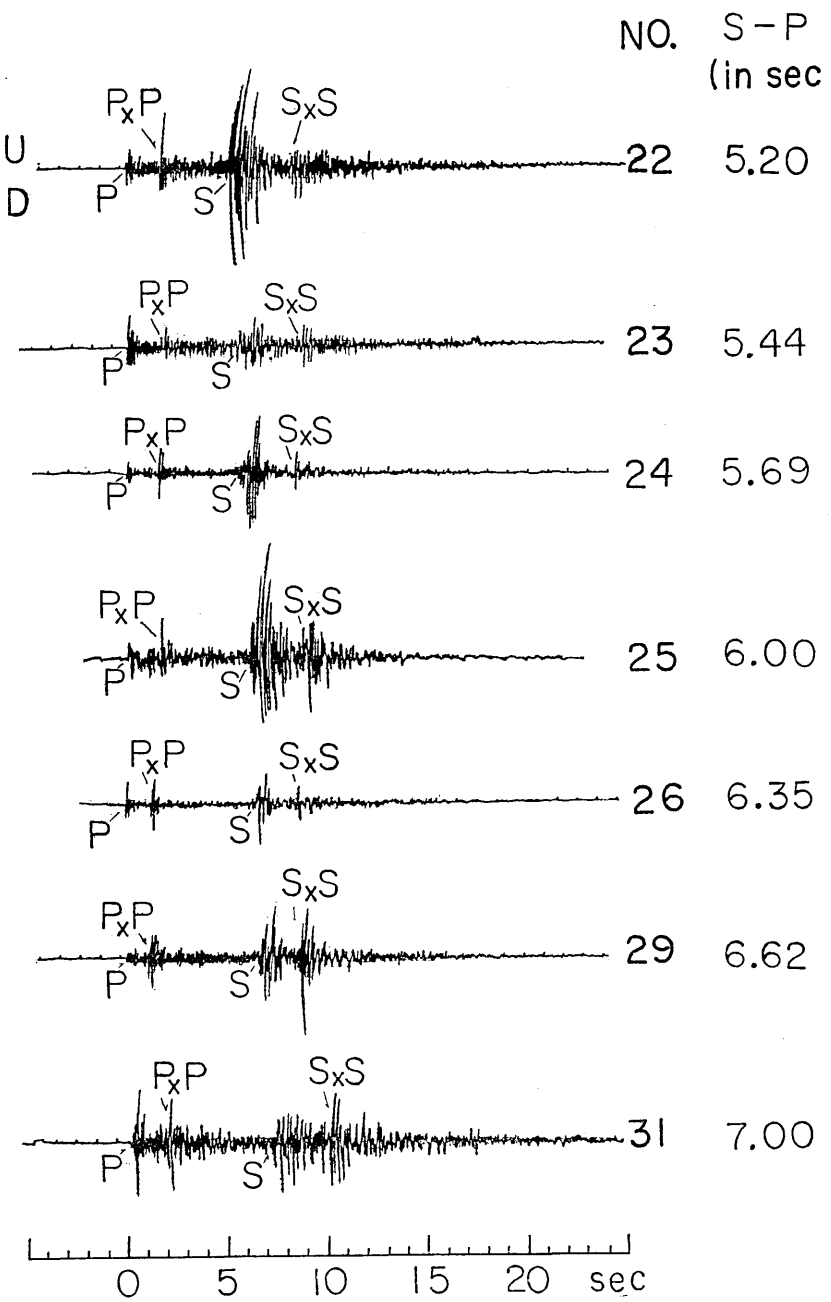

Fig. 8. Vertical component seismograms at Sarutani station reproduced from the herical drum records with paper speed of 4 mm/sec. The *P* and *S* reflections from the Conrad discontinuity are denoted as *PxP* and *SxS*. Numbers for the reproduced seismograms correspond to those in Table 3.

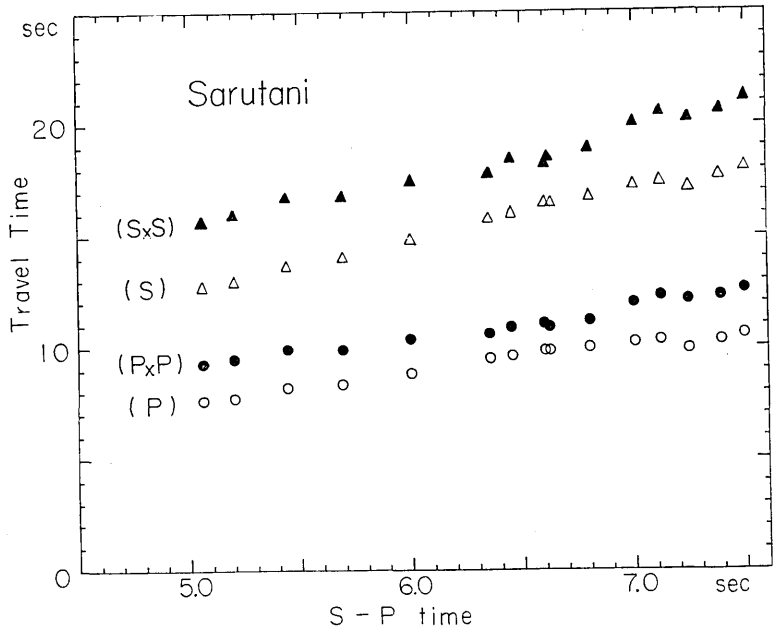

Fig. 9. Observed travel times of P, PxP, and SxS versus $S-P$ time relations at Sarutani stations.

seconds. Though reexaminations will be necessary for the immediate comparisons of the amplitude ratios as deduced from the horizontal component seismograms with those from the vertical ones, the abrupt increase in the amplitude ratios at the distance larger than about 5.0 seconds in the S minus P interval will possibly be associated with the expected increase in the reflection coefficient of the seismic wave energy at the critical distance range. Relations of the travel time versus the S minus P interval are plotted in Fig. 9 for the direct P, S, PxP and SxS phases on the basis of the time readings of the records at Wk and St stations.

Data from 31 earthquakes listed in Table 3 are plotted on the graph in Fig. 10 which covers the S minus P interval of 0.6–7.5 seconds. As shown in Fig. 3, all the foci of the earthquakes used are projected onto the vertical north-south and east-west sections. The focal depths of the events range from 3 to 12 km.

Theoretical curves for the SxS reflections from a horizontal velocity discontinuity at a depth (H_1) of 24 km are also drawn in Fig. 10 as the best fitting result to the observational data for the S minus P interval ranging 0–4.0 seconds. Two curves for each reflected phase are given, one for a 3 km depth of focus (h), the other for a 12 km depth of focus. The left hand ends of each curve are theoretical limits of observable reflections at the specified depth of focus. The

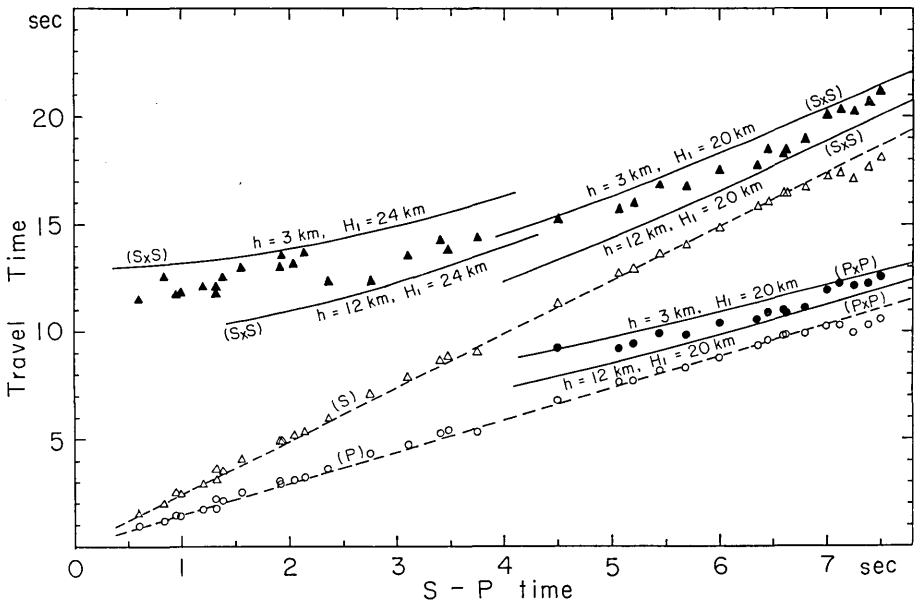

Fig. 10. Observed and theoretical travel times of P, S, PxP and SxS versus $S-P$ time. All curves are computed using a P velocity of 5.80 km/sec and S velocity of 3.46 km/sec.

theoretical curves were computed using the S velocity of 3.46 km/sec. As resulted from the time distance relations, the depth of the Conrad discontinuity (H_1) can be estimated as 24 km in the west coast area around Wakayama city designated as (A) in Fig. 1. Theoretical curves for both PxP and SxS reflections from a horizontal discontinuity at a depth (H_1) of a 20 km are also drawn in Fig. 10 as the best fitting result to the observational data for the S minus P interval ranging 4.0–7.5 seconds. In general, only one combination of (h) and (H_1) values will produce theoretical curves that fit the PxP and SxS data equally well. The theoretical curves were computed using the P wave velocity of 5.8 km/sec and the S wave velocity of 3.46 km/sec respectively. In this particular case, the theoretical curves bracketed both PxP and SxS data in about the same way, so that little adjustment in the values of (h) and (H_1) is possible. From the time distance relations thus obtained, the depth of the Conrad discontinuity (H_1) can be estimated as 20 km in the inland area (B) adjacent to the coastal area (A). An inclination dipping to the west of the Conrad discontinuity can be expected to have approximate gradient of 1/10 as derived from the difference in the value of (H_1) between the two areas of (A) and (B). Theoretical travel time curves for the direct P and S waves are also drawn in Fig. 10 in case of the representative value of focal depth

of 7 km using the P wave velocity of 5.80 km/sec and the S wave velocity of 3.46 km/sec.

By taking the value of (H_1) as 20 km and the velocities in the lower crustal layer as 6.80 km/sec for the P waves and 4.05 km/sec for the S waves as given in the next section, the calculated critical distance Δ_1, at which an increase in amplitudes of the reflections being expected, is 60.5 km ($S-P$ interval=7.07 sec) for $h=3$ km, 53.9 km ($S-P$ interval=6.34 sec) for $h=7$ km and 45.8 km ($S-P$ interval=5.5 sec) for $h=12$ km respectively. The corresponding critical angle of emergency e_1 is 58°32′. The calculated distance ranges are harmonious with the observed results.

Reflections from the Mohorovičić Discontinuity

A preliminary result as to the thickness of the earth's crust in the Kii Peninsula will be represented in this section on the basis of the observed data of the seismic wave reflections from the Mohorovičić discontinuity as well as those from the Conrad discontinuity as mentioned in the previous section. At distances from epicenters, where critically reflected waves may be expected, observations of well located earthquakes will provide a set of data available for the study of the time distance relations of the reflected waves. The reflected phases from the Mohorovičić discontinuity designated as P_MP, which follow the direct P by about 1.4 and 2.3 seconds, and S_MS, which follow the direct S by about 1.6 and 3.6 seconds, are observed at Hb (Haibara) station

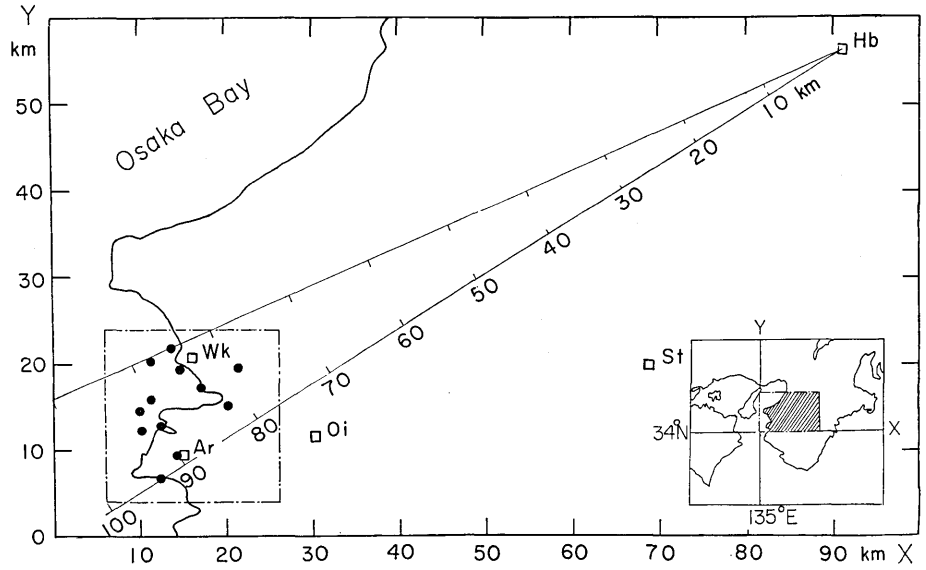

Fig. 11. Epicentral distributions of earthquakes listed in Table 4.

Table 4. List of earthquakes used for the travel time analysis of the Moho reflections of P_MP and S_MS as arranged in order of epicentral distances. (Epicentral coordinates of X and Y are measured in km as positive to the east and to the north respectively, from the origin of 135°E and 34°N. Focal depth measured in km is denoted as Z.)

No.	Date	Origin Time			Hypocentral Coordinates (km)			Mag.	Distance (km)	Travel Time in sec			
		h	m	s	X	Y	Z			$P-O$	P_MP-O	$S-O$	S_MS-O
1	Sep. 03, 1969	06	06	42.73	21.26	19.73	2.49	3.2	78.9	13.30	15.55	22.76	26.30
2	Aug. 29, 1969	18	31	58.08	20.23	15.16	3.60	3.2	82.0	13.51	15.51	23.53	26.27
3	Mar. 02, 1969	04	21	32.70	16.96	17.27	4.64	3.5	83.9	13.96	15.92	23.73	27.06
4	Feb. 13, 1969	01	33	08.06	13.71	21.82	6.14	3.8	84.8	14.34	16.56	24.34	27.49
5	May 18, 1969	10	14	40.97	14.58	19.40	4.69	3.4	85.0	14.39	16.54	24.69	27.38
6	Jan. 11, 1968	20	22	32.82	11.29	20.38	6.19	3.2	87.6	14.71	16.56		
7	Feb. 02, 1969	01	16	49.15	11.25	16.02	6.08	3.1	89.5	15.07	17.07	25.82	28.07
8	Aug. 07, 1969	21	25	39.33	12.54	12.89	5.78	2.8	89.8	14.92	16.87	25.92	28.12
9	Jan. 17, 1967	07	20	17.71	9.97	14.55	6.66	3.0	91.3	15.88	17.64	26.48	29.38
10	Sep. 02, 1967	20	08	30.90	10.20	12.29	7.35	3.1	92.2	15.60	17.35		
11	Jan. 29, 1969	16	52	39.66	12.27	6.61	5.37	3.5	93.2	15.89	17.34	26.89	28.49
12	Dec. 29, 1967	22	00	10.05	10.03	7.76	8.04	3.1	94.5	16.30	17.85	27.90	29.70

about 78–95 km from epicenters of the earthquakes in the area enclosed by the square in Fig. 11. List of 12 earthquakes used is arranged in order of the epicentral distances as listed in Table 4. Seismograms are reproduced in Fig. 12 from the original herical drum records of vertical component seismograph at Hb station. Magnification and sensitivity of the seismograph at Hb station is given in Table 2. Data from 12 earthquakes listed in Table 4 are plotted on the graphs in Fig. 13 representing the relations of the travel time of P, P_MP and S_MS versus epicentral distance in the range of 78–95 km.

At Hb station, the reflected phases P_MP and S_MS can be detected for about 80% of earthquakes with magnitude M of more than 3.0 as located in the enclosed area in Fig. 11. On the other hand, however, at both the two stations of Sk and Ku, it is a rare case for prominent reflections to be observed. The difference of frequency in the presence of the reflections at these stations may supposedly be caused

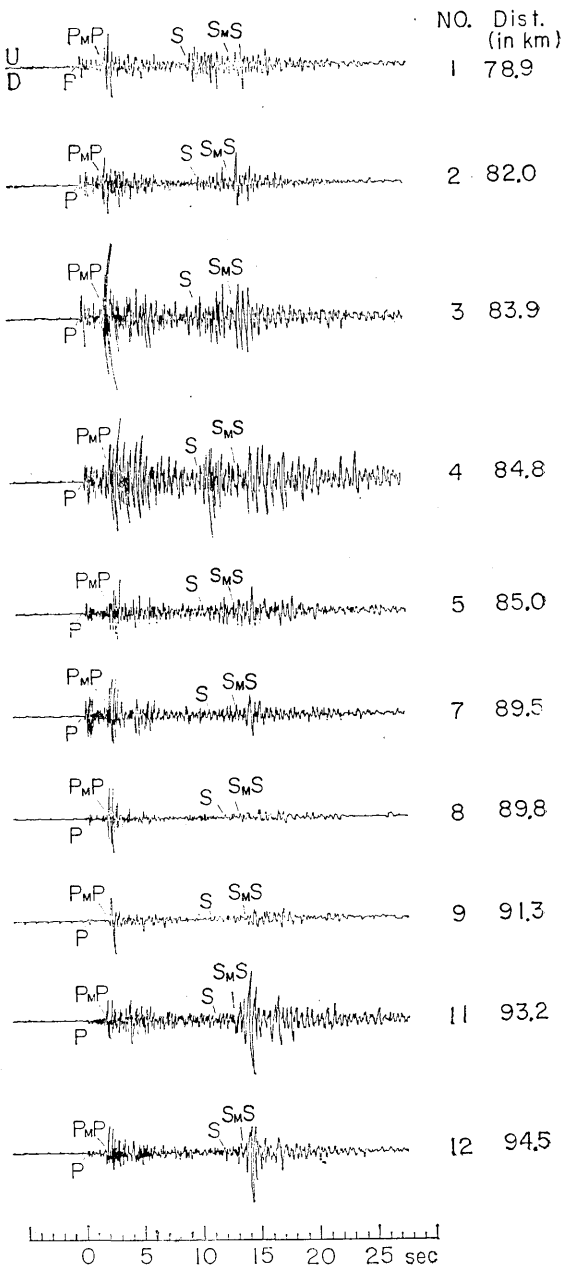

Fig. 12. Vertical component seismograms at Hb station reproduced from the herical drum records with paper speed of 4 mm/sec. The P and S reflections from the Mohorovičić discontinuity are denoted as P_MP and S_MS. Numbers for the reproduced seismograms correspond to those in Table 4.

mainly by the azimuthal variations in energy radiation of the seismic waves at the focus and also by the local difference in the reflection coefficient related with the sharpness of the discontinuity in the earth's crust. The effects on amplitudes above mentioned should be reserved for future studies with special concern to amplitude analysis.

In the case of the crustal model with two horizontal layers, travel time (T) and epicentral distance (Δ) are in the following relations for the reflections from the Mohorovičić discontinuity, i.e.,

$$T=\frac{2H_1-h}{V_1\cos i_1}+\frac{2H_2}{V_2\cos i_2}\,, \tag{1}$$

$$\Delta=(2H_1-h)\tan i_1+2H_2\tan i_2\,, \tag{2}$$

and

$$\frac{\sin i_1}{V_1}=\frac{\sin i_2}{V_2} \tag{3}$$

where, (V_1) and (V_2) denote the velocities in the upper and lower layers of the earth's crust with each thickness of (H_1) and (H_2) respectively. Let (i_1) and (i_2) be the incident angles of a seismic ray at the interface of a depth of (H_1). Then we have a theoretical travel time curve for reflected waves from the Mohorovičić discontinuity for a given crustal model assuming a focal depth of h less than (H_1).

As described in the previous section, the P wave velocity (V_{P_1}) is 5.80 km/sec and the S wave velocity (V_{S_1}) is 3.46 km/sec in the upper crustal layer. The depth of the Conrad discontinuity simultaneously given is 24 km in the west coast area of (A) and 20 km in the inland area (B) adjacent to the former (Fig. 1). Time distance relations are calculated in the case of $H_1=20$ km, because a seismic ray is reflected from the Mohorovičić discontinuity in the area (B) for the earthquakes used at present. Then, the combination of (H_2) and (h) values will produce a theoretical travel time curves which fit the P_MP and S_MS data equally well when we assume the most probable velocity values of (V_2) designated as (V_{P_2}) for the P waves and (V_{S_2}) for the S waves.

As the best fitting result, the theoretical curves for the P_MP and S_MS reflections in the case of $H_2=10$ km, $V_{P_2}=6.8$ km/sec and $V_{S_2}=4.05$ km/sec are drawn in Fig. 13. Two curves for each reflected phase are given, one for a 3 km depth of focus (h), the other for a 10 km depth of focus corresponding to the upper and lower limits of the focal depths of the earthquakes used. Comparing the theoretical curves with the observational data plots in Fig. 13, the crustal model proposed in this section is the best interpretation of the time distance data of the P_MP and S_MS, inasmuch as the value of focal depth (h) for the theoretical

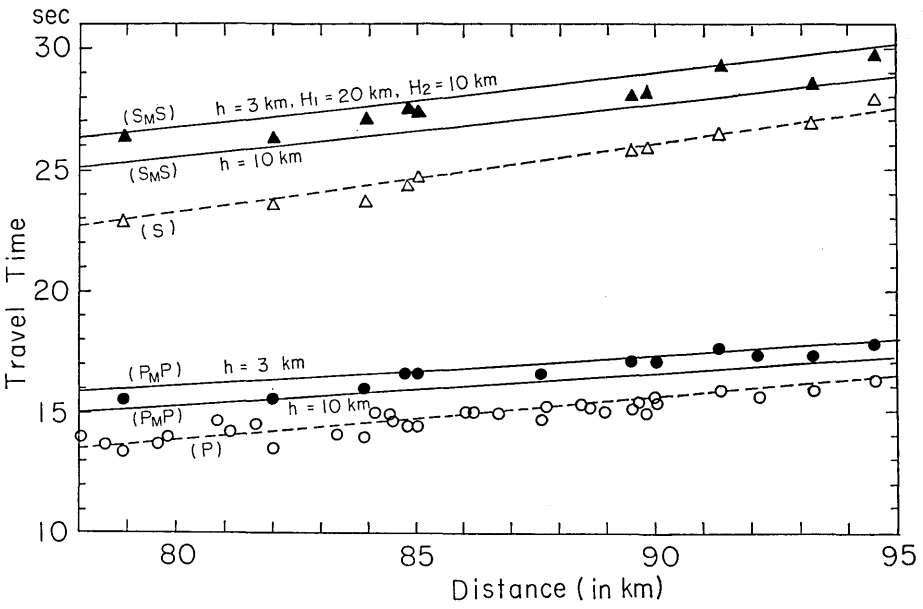

Fig. 13. Observed and theoretical travel times P, P_MP, S and S_MS versus $S-P$ time at Hb station. P time data at Sk and Ku stations are plotted simultaneously.

curves are in good agreement with the distribution of depth of focus. The critical distance Δ_2 for the reflections from the Mohorovičić discontinuity is given as 69.5 km in the case of $h=7$ km when we take the Pn velocity of 7.9 km/sec as given in the next section. Thus the distance range under investigation can be included in the critical distance range of the Mohorovičić reflections. In addition to the results, it should be noted that the observational data plots in Fig. 13 for the direct P and S waves at the distance range of 78–95 km are harmonious with the theoretical travel time curves related with the velocities of $V_{P_1}=5.80$ km/sec and $V_{S_1}=3.46$ km/sec as given in the previous section.

Travel Times of the *Pn* and *Pg*

In combination with the hypocentral coordinates determined by J.M.A. (Japan Meteorological Agency), the apparent velocities of the Pn and Pg phases are calculated from the arrival time data provided by the network observations at Wakayama Micro-earthquake Observatory. Observed critical distance Δ_{CR}, at which the Pn phase becomes the first break, is compared with that from theoretical travel time curves.

On Sept. 9, 1969, a destructive earthquake named the Okumino Earthquake, occurred in the middle part of Gifu Prefecture, Central

Japan. J.M.A. reported the following result of the origin of the event[12], i.e.,

Origin Time = $14^h15^m33^s.5 \pm 0^s.2$ (in Japan Standard Time)

Latitude = 35°47'N ± 01', Longitude = 137°04'E ± 01',

Focal Depth $h = 0$ km, Magnitude $M = 6.6$.

Informations of the origins of the major aftershocks associated with the event were also reported by J.M.A.[12]

Table 5. Travel times of *Pn* and *Pg* phases in relation to the epicentral distance for the aftershocks of the Okumino Earthquakes located at the middle of Gifu Pref.

No. 1. Date=Sep. 10, 1969, Origin time=$21^h03^m14^s.8 \pm 0^s.2$
Lat.=35°50'±01', Long.=138°01'±01', H=10 km, M=4.3

Station	Distance	Pn		Pg
				m s
Is	154.48 km	+*iP*	$21^h\ 03^m\ 41^s.97$	
In	164.48	+*eP*	43.30	
Hb	174.77	+*iP*	44.89	
St	217.91	+*eP*	50.00	03 53.2
Ku	225.11	*eP*	50.8	53.5
Oi	246.21	+*eP*	54.3	58.3
Kk	258.68	*eP*	54.9	59.6
Ar	257.53	+*iP*	55.65	
Hd	272.62	+*iP*	57.1	04 01.5
Sk	277.56	*eP*	57.3	

No. 2. Date=Sep. 17, 1969, Origin Time=$06^h28^m35^s.5 \pm 0^s.2$
Lat.=35°50'±01', Long.=137°08'±01', H=10 km, M=3.8

Station	Distance	Pn		Pg
				m s
Is	143.69 km	+*eP*	$06^h\ 29^m\ 00^s.20$	
In	157.20	+*iP*	02.10	
Hb	170.20	+*eP*	04.02	
St	213.22	+*eP*	09.14	29 12.3
Ku	217.83	*eP*	09.85	13.1
Oi	243.35	+*eP*	13.3	17.8
Kk	254.38	*eP*	14.3	19.0
Ar	255.35	*eP*	14.9	19.8
Hd	269.80	+*eP*	16.2	22.2
Sk	271.01	*eP*	16.2	

12) Japan Meteorological Agency, *The Seismological Bulletin of the Japan Meteorological Agency* for September 1969.

Table 5. (Continued)

No. 3. Date=Sep. 20, 1969, Origin Time=$03^h59^m39^s.8\pm0^s.1$
Lat.=35°46′±01′, Long.=137°06′±01′, H=10 km, M=4.0

Station	Distance	Pn		Pg
				m s
Is	148.46 km	+eP	$04^h00^m05^s.48$	
In	160.93	+iP	07.29	
Hb	172.85	+iP	08.84	
St	215.96	eP	13.9	00 17.9
Ku	221.44	eP	14.70	17.3
Oi	245.43	+eP	18.25	22.5
Kk	257.01	iP	18.82	23.8
Ar	257.18	+eP	19.70	24.7
Hd	271.87	eP	21.0	26.7
Sk	274.42	eP	21.2	

No. 4. Date=Sep 21, 1969, Origin Time=$08^h41^m29^s.4\pm01$
Lat.=35°47′±00′, Long.=137°06′±01′, H=10 km, M=3.9

Station	Distance	Pn		Pg
				m s
Is	150.26 km	+iP	$08^h\ 41^m\ 55^s.38$	
In	162.67	+iP	57.20	
Hb	174.37	+iP	59.24	
St	217.46			
Ku	223.14	+iP	42 04.95	42 08.1
Oi	246.82	+eP	08.6	12.4
Kk	258.49	+iP	09.6	13.8
Ar	258.54	eP	09.9	14.4
Hd	273.25	eP	11.0	16.8
Sk	276.05	eP	11.5	

Seismological network of Wakayama Micro-earthquake Observatory covers the distance range of about 150–280 km from the epicenters of the aftershocks. The prominent Pg phase was registered after the initial Pn phase by 2–5 seconds at the stations of the network. Travel time analysis is made for the selected 4 events listed in Table 5, the time readings of which are within the limit of error of ±0.02 seconds for the initial Pn phase and ±0.04 seconds for the later Pg phase. Seismograms of the earthquakes used are arranged in time distance relations as exemplified in Fig. 14a-d reproduced from the original herical drum records of vertical component seismographs at the representative 8 stations.

Arrival time readings at Wk station, located in the urban area of Wakayama city, are excluded from the group of analyzed data because of the insufficient accuracy in the arrival time readings of the phases

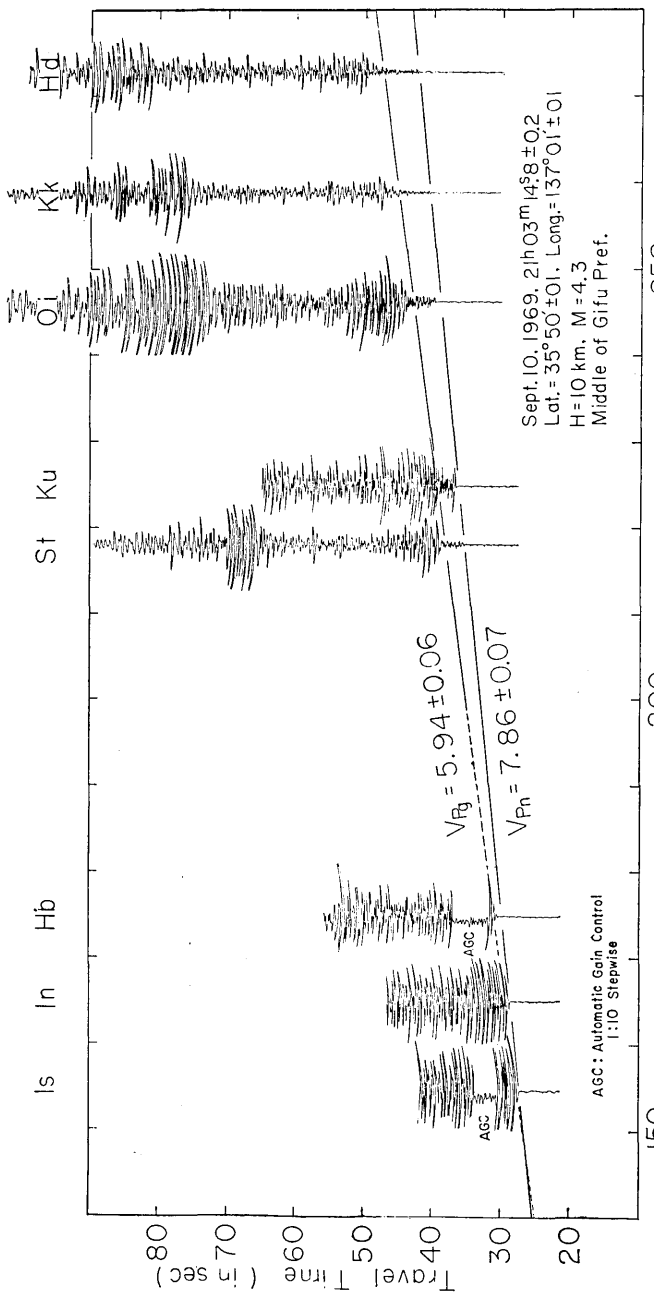

Fig. 14-a. Reproduced seismograms of the earthquake No. 1 in Table 5 with *Pg* and *Pn* phases.

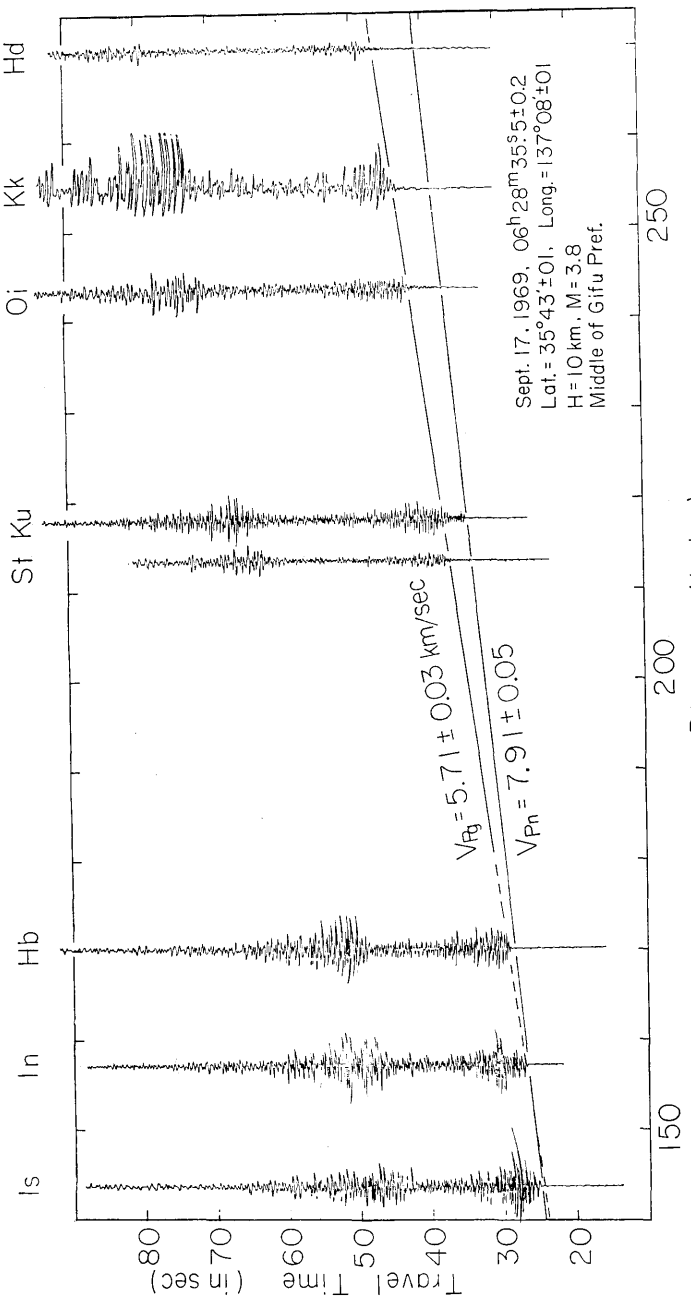

Fig. 14-b. Reproduced seismograms of the earthquake No. 2 in Table 5 with *Pg* and *Pn* phases.

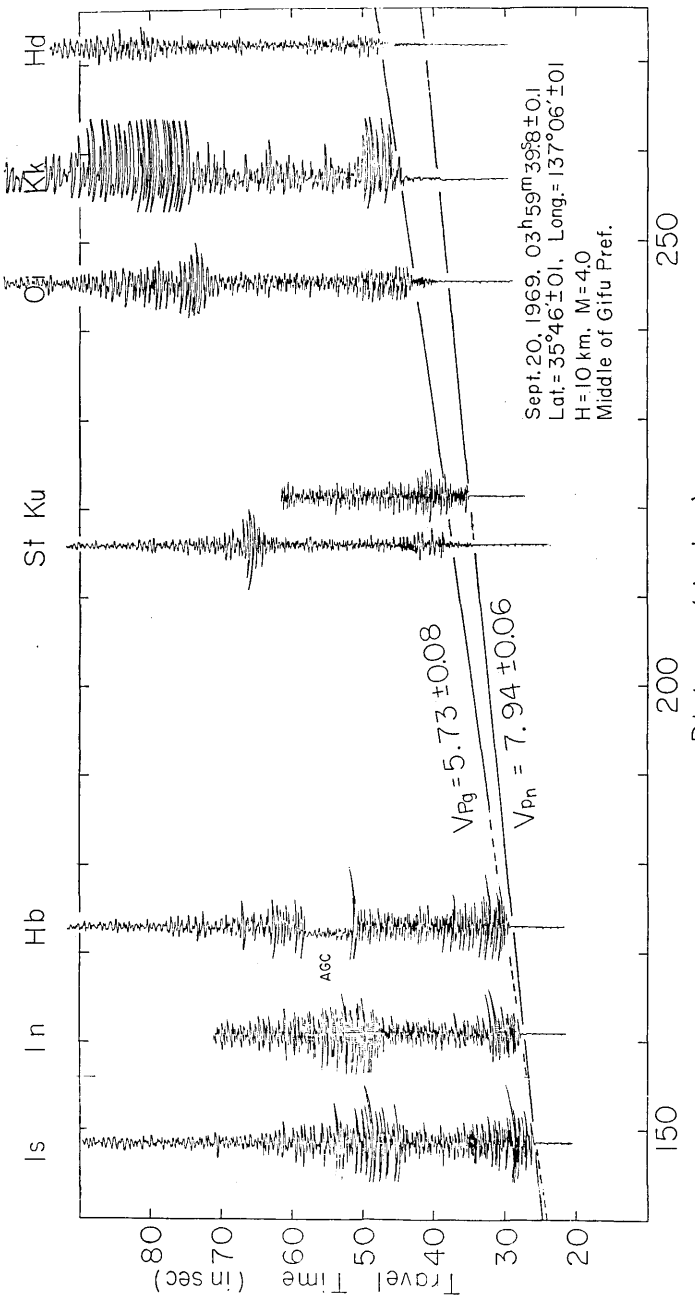

Fig. 14-c. Reproduced seismograms of the earthquake No. 3 in Table 5 with *Pg* and *Pn* phases.

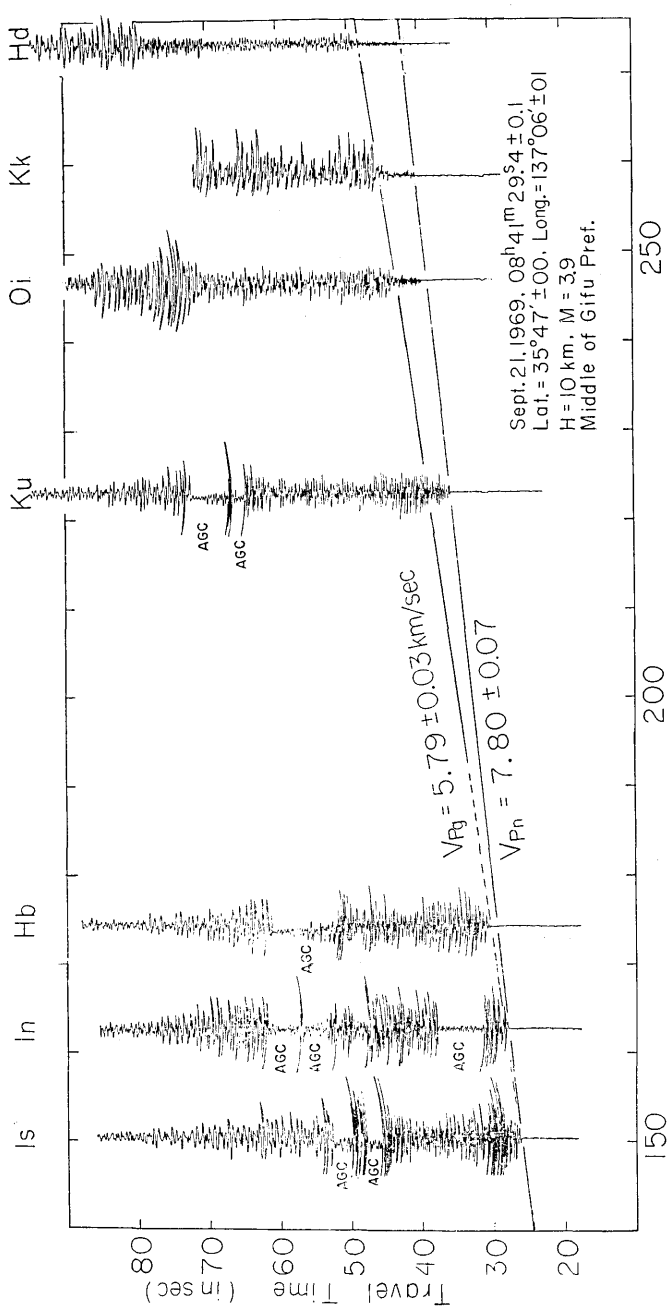

Fig. 14-d. Reproduced seismograms of the earthquake No. 4 in Table 5 with *Pg* and *Pn* phases.

detected by the relatively low magnification seismographs of the station. It is almost impossible to identify the *Sn* phase separately from the superimposed signals with high frequency components due to too small amplitudes of the *Sn* phase on the records of the vertical component seismographs at the stations. In regard to the *Sg* phase, the difficulties in making accurate measurements of arrival times arise from the gradual increase of both amplitudes and frequencies of the seismic signals with time. In this connection, traval time study is restricted to that of the *Pn* and *Pg* phases at present.

The apparent velocities of the *Pn* and *Pg* phases, designated as V_{Pn} and V_{Pg} respectively, are estimated from the observed time distance relations through the least square procedures as shown in Fig. 15. Averaged values of the V_{Pn} and V_{Pg} are determined as 7.9 ± 0.1 km/sec and 5.8 ± 0.1 km/sec respectively. The value of the V_{Pg} obtained here is in good agreement with the values of the *P* wave velocity in the upper crustal layer as derived from the travel time curves of the reflections *PxP* and the direct *P* waves at the near distance range of the *S* minus *P* interval of less than 7.5 seconds.

In the case of the crustal model with two horizontal layers, the critical distance Δ_{CR}, at which the *Pn* phase becomes the first break, is written in the form of

$$\Delta_{CR}=\frac{(2H_1-h)(V_{P_3}^2-V_{P_1}^2)^{1/2}}{V_{P_3}-V_{P_1}}+\frac{2H_2(V_{P_3}^2-V_{P_2}^2)^{1/2}}{V_{P_3}-V_{P_1}}\left(\frac{V_{P_1}}{V_{P_2}}\right), \qquad (4)$$

when the conditions for a focal depth of (h) as given $h<H_1$ and $h\leqslant\Delta_{CR}$ are satisfied. In Eq. 4, (V_{P_1}) and (V_{P_2}) denote the velocities in the upper and the lower layers of the earth's crust with each thickness of (H_1) and (H_2) respectively. The velocity (V_{P_3}) can be taken to be equal to (V_{Pn}) at present. For the crustal model in the inland area of (B), the following values can be applied, i.e., $V_{P_1}=5.8$ km/sec, $V_{P_2}=6.8$ km/sec, $V_{P_3}=7.9$ km/sec, $H_1=20$ km and $H_2=10$ km.

The focal depth (h) of the earthquakes used is determined by J. M.A. in the discrete values of a 10 km depth classification. The value of (h) given by J.M.A. is, however, open to the possibility of reduction to a value less than 10 km considering the results from the close distance observation carried out by H. Watanabe and A. Kuroiso.[13]

The calculated critical distance (Δ_{CR}) is in the range of 109–135 km corresponding to the focal depth range of 0–10 km as derived from Eq. 4 in the case of the crustal model proposed at present. On the other hand, observational data in Fig. 15 indicate that the critical distance

13) H. WATANABE, and A. KUROISO, "Aftershocks of the Earthquake of the Central Part of Gifu Prefecture, September 9, 1969," *Bull. Earthq. Res. Inst.*, **48** (1970), 1195-1208.

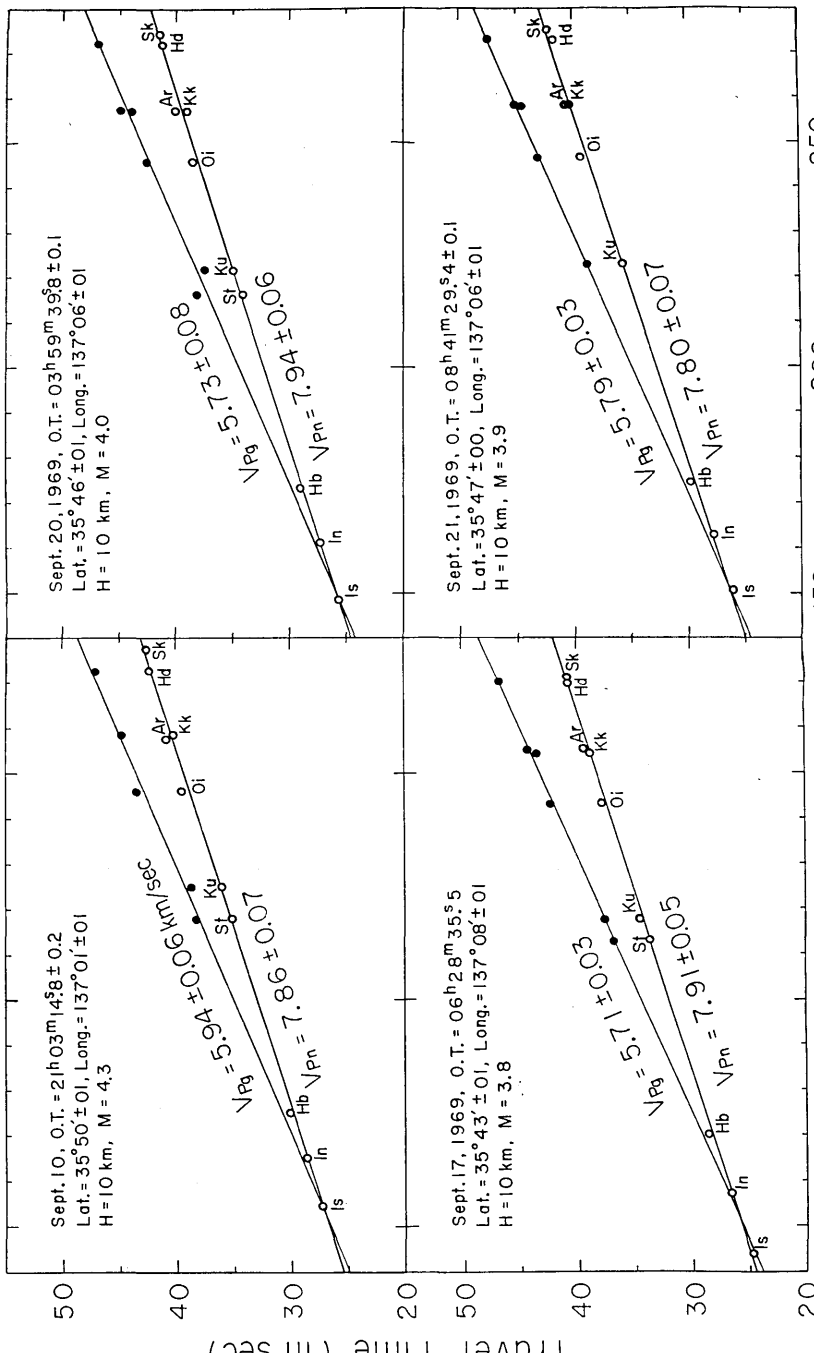

Fig. 15. Observed travel times of *Pg* and *Pn* versus epicentral distance for the earthquakes listed in Table 5.

(Δ_{CR}) ranges in the distance of 145–155 km. The discrepancy found in the calculated and observed values of (Δ_{CR}) may be attributable to the difference in the thickness of the earth's crust between the two areas of (B), included in the network area, and (C) outside it. Despite the fact that no information is available for the crustal reflections in the area of (C), a possible way to interpret the discrepancy in the values of (Δ_{CR}) is to introduce a larger value of 18 km for (H_2) in the area of (C) than that of 10 km for (H_2) in the area of (B).

Conclusion

Time distance relations of the deep crustal reflections were investigated in terms of the crustal structure in the Kii Peninsula, Central Japan on the basis of the observational data detected at Wakayama Micro-earthquake Observatory. In order to evaluate the seismic wave velocities in the earth's crust, time distance data of the direct and refracted waves were correlated with the data of the reflections.

In addition to the direct P and S phases, the nearby earthquakes (S minus P interval$\leq$4.0 seconds) recorded at Wk (Wakaura) and Oi (Oishiyama) stations have a sharp later arrival which follows the direct S phase by about 5 and 11 seconds. The later arrival can be identified as the subcritical S phase reflections designated as SxS from the Conrad discontinuity. For the larger distance range of the S minus P interval of 4.5–7.5 seconds, two sharp arrivals detected at Wk and St (Sarutani) stations, one of which follows the direct P phase by about 1.0 and 2.4 seconds and the other the direct S phase about 1.9 and 3.9 seconds, are also identified as the critical P and S phase reflections designated as the PxP and SxS from the Conrad discontinuity. The reflections of the P and S phases from the Mohorovičić discontinuity designated as the P_MP, which follows the direct P phase by about 1.4 and 2.3 seconds, and S_MS, which follows the direct S phase by about 1.6 and 3.6 seconds, are also observed at Hb (Haibara) station in the epicentral distance range of 78–95 km.

The best interpretation of the time distance relations for the reflections is that the depth of the Conrad discontinuity can be measured as 20–24 km in the western part of the Kii Peninsula with a possible inclination dipping to the west. The depth of the Mohorovičić discontinuity can be estimated as about 30 km in the inland area of the western part of the Kii Peninsula. The seismic wave velocities in the upper and the lower crustal layers are determined as 5.80 km/sec and 6.80 km/sec for the P-waves and 3.46 km/sec and 4.05 km/sec for the S-

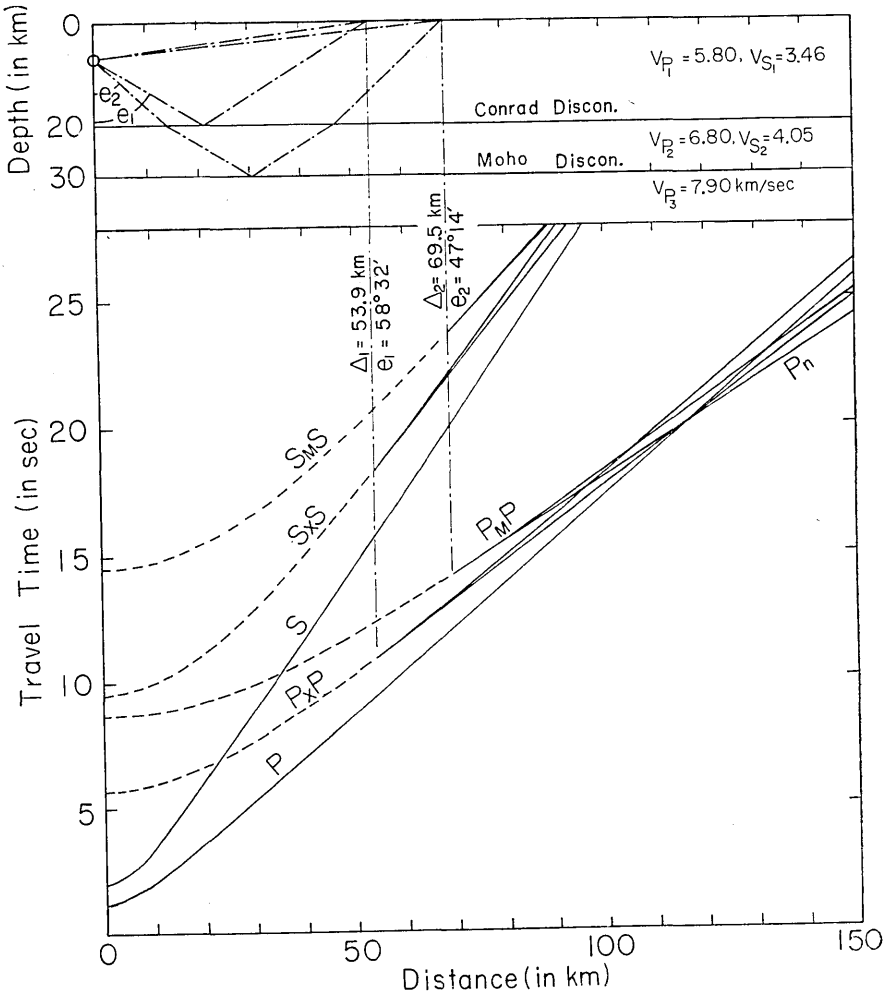

Fig. 16. Theoretical travel time curves related with the crustal model obtained.
Δ_1; Critical distance for the Conrad reflections.
e_1; Critical emergency angle for the Conrad reflections.
Δ_2; Critical distance for the Moho reflections.
e_2; Critical emergency angle for the Moho reflections.

waves respectively. The velocities of the *Pg* and *Pn* waves are determined as 5.8 km/sec and 7.9 km/sec from the arrival times at the stations of the network in combination with the locations of the aftershocks associated with the Okumino Earthquake in Sept. 9, 1969, determined by J.M.A. (Japan Meteorological Agency).

As reduced from the crustal model obtained at present, travel time curves in the distance range of 0–150 km are shown in Fig. 16 in the case of a focal depth $h=7$ km. The critical distances and the angles of emergency in this case are 53.9 km and 58°32′ for the Conrad re-

flections and 69.5 km and 47°14′ for the Mohorovičić reflections.

Acknowledgements

The writer wishes to thank Prof. S. Miyamura for his important comments and suggestions regarding this work.

---

4. 和歌山微小地震観測所およびその衛星観測点で観測された地震反射波および屈折波の走時と地殻構造

地震研究所　溝　上　　恵

和歌山微小地震観測所の定常観測資料にもとづいて地殻内部の不連続面での反射波および屈折波の走時解析を行ない紀伊半島の地殻構造との関係を調べた．以下その結果を要約する．

1) 和歌浦観測点および生石山観測点において S-P time が 4 秒以下の浅い地震（震源の深さが約 4-10 km）を観測すると水平動成分に直達 S 波より約 5-11秒おくれて顕著な位相がしばしば検出される．その走時から判定すると，これは Conrad 不連続面での S 波の Subcritical Reflection SxS である．

2) 和歌浦観測点および猿谷観測点において S-P time が，4.5-7.5 秒の浅い地震を観測すると直達 P 波より約 1.0-2.4 秒おくれて 1 つの顕著な位相が検出される．さらに直達 S 波より約 1.9-3.9 秒おれて別の顕著な位相が検出される．それらの走時から判定すると，これら 2 つの位相はそれぞれ Conrad 不連続面での P 波および S 波の Critical Reflection PxP および SxS である．

3) 1) および 2) の観測結果から求められる走時曲線を解析すると，紀伊半島西岸地域 (Fig. 1 の A 地域) および内陸部 (Fig. 1 の B 地域) で Conrad 不連続面の深さは，それぞれ 24 km および 20 km となる．これは Conrad 不連続面が内陸部から西岸地域へ平均 1/10 の勾配で傾斜していることに対応する．地殻上部層（地表から Conrad 不連続面まで）の平均的な P 波および S 波の速度は，それぞれ 5.80 km/sec および 3.46 km/sec である．

4) 榛原観測点において震央距離 78-95 km にある浅い地震を観測すると直達 P 波より約 1.4-2.3 秒おくれて 1 つの顕著な位相が検出される．さらに直達 S 波より約 1.6-3.6 秒おくれて，別の顕著な位相が検出される．それらの走時から判定すると，これら 2 つの位相はそれぞれ Moho 不連続面での P 波および S 波の Critical Reflection P_MP および S_MS である．

5) 3) の解析結果と 4) の観測結果から求められる走時曲線とを同時に考慮すると紀伊半島内部 (Fig. 1 の B 地域) Moho での不連続面の深さは約 30 km である．地殻下部層 (Conrad 不連続面から Moho 不連続面まで) の平均的な P 波および S 波の速度はそれぞれ 6.80 km/sec および 4.05 km/sec である．

6) 1969 年 9 月 9 日に岐阜県中部に発生した，奥美濃地震 (M=6.6) の余震の走時解析から求められる Pg 波および Pn 波の見かけ速度はそれぞれ 5.9 km/sec および 7.9 km/sec である．ここで得られた Pg 波の見かけ速度は，反射波 PxP の走時から得られた地殻上部層の平均的速度と一致する．

7) 奥美濃地震の余震の走時解析によると，Pn 波が初動として観測される最小の震央距離 Δ_{CR} は 145-155 km である．一方，紀伊半島内陸部 (Fig. 1 の B 地域) の地殻構造から推定すると，震源の深さ 0-10 km の地震について Δ_{CR} は 109-135 km となる．両者の差は，奥美濃地震の余震域から紀伊半島北部までの地域 (Fig. 1 の C 地域を含む) の平均的な Moho の深さが紀伊半島内部のそれよりも約 8 km 深く，地殻の厚さが約 38 km であるとすれば説明できる．

8) 3) および 5) に記した地震波速度を用いかつ Conrad 不連続面の深さおよび Moho 不連続面の深さをそれぞれ 20 km および 30 km とすると，震源の深さが 7 km の地震について Conrad 反射波の Critical Distance Δ_1 は 53.9 km (S-P time=6.34 sec)，それに対応する地震波の震源での射出角 e_1 は 58°32′ である．また Moho 反射波については Critical Distance Δ_2 が 69.5 km 射出角 e_2 が 47°14′ となる．